



Synthesis of Ag nanowires with an aspect ratio higher than 2000 for the fabrication of transparent conductive film

Hezheng Ao¹, Junyan Feng^{2,*} , Peng Cao¹, Tao Yang¹, Tao Shang³, and Bo Xing^{3,*}

¹ College of Mechanical Engineering, Zhejiang University of Technology, Hangzhou 310014, Zhejiang, China

² College of Mechanical and Electronic Engineering, Jiaying Nanhu University, Jiaying 314001, China

³ College of Information Science and Engineering, Jiaying University, Jiaying 314000, China

Received: 5 July 2023

Accepted: 1 November 2023

Published online:
18 November 2023

© The Author(s), under exclusive licence to Springer Science+Business Media, LLC, part of Springer Nature, 2023

ABSTRACT

Silver nanowires (AgNWs) are promising materials in the fabrication of flexible and transparent conductive thin films (FTCFs), which are key components of flexible optoelectronic devices. However, the performance of AgNW FTCFs is severely limited by their low aspect ratio, and the fabrication of AgNWs with a high aspect ratio remains a significant challenge. In this study, AgNWs with a diameter of 40 nm and aspect ratio of 2000 were synthesized rapidly by controlling the total molar concentration of Cl^- ions in the reaction solution by a typical polyol method to adjust the $\text{Cu}^{2+}/\text{Fe}^{3+}$ molar ratio. Subsequently, AgNW FTCFs were fabricated by the coating method using hydroxyethyl cellulose (HEC). The films exhibited a low sheet resistance of $68 \Omega/\text{sq}$ and transmittance of 86.70%, which are comparable to those of typical indium tin oxide electrodes. Meanwhile, a mechanical robustness test showed that the sheet resistance of the AgNW-HEC films increased by only 3.15% even after 3000 bending cycles.

1 Introduction

In recent years, owing to their high transmittance, low sheet resistance, and high flexibility, flexible and transparent conductive films (FTCFs) are being used widely as electrodes in sensors [1], touch screens [2], solar cells [3], organic light-emitting diodes [4, 5], and human-machine interfaces [6]. However, owing to the scarcity of indium and the complexity of its manufacturing process, indium tin oxide (ITO) has become increasingly expensive. In addition, its inherent brittleness hinders its applicability in flexible devices,

because these devices require not only a high transparency and conductivity but also good mechanical flexibility. Therefore, alternatives are being explored to replace ITO. These include graphene [7–10], carbon nanotubes [11, 12], conductive polymers [13], and metal nanowires (NWs) [14, 15], such as those of Ag and Cu. Among the various materials being investigated, metallic networks, especially AgNW networks [16], are regarded as the ideal replacements for ITO because of their excellent optical transmittance and high electrical conductance.

Address correspondence to E-mail: 202408@jxnhu.edu.cn; xingbo@zjxu.edu.cn

A few studies have suggested that the use of ultralong AgNWs with high aspect ratios is a promising strategy for improving the performance of FTCFs. The smaller the diameter and greater the length of the NWs, the longer the penetration path and the lower the number of high-resistance wire–wire contacts in the film. This, in turn, results in a network with a lower number density of wires and lower contact resistance. Studies have also suggested that the length and diameter of the NWs have a determining effect on ensuring high transparency with low haze [17–20]. Therefore, extending the length of the NWs and keeping their diameter as small as possible constitutes a simple solution to overcome several challenges related to the large-scale applicability of AgNWs. Many chemical techniques have been developed for the synthesis of AgNWs, including template-directed synthesis [21], the electrochemical technique [22, 23], ultraviolet-irradiation-based photoreduction [24], hydrothermal and solvothermal methods [25, 26], and polyol synthesis [27]. The polyol process remains one of the most promising methods because of its simplicity and high yield. Typically, polyvinylpyrrolidone (PVP) is used as the capping agent, and ethylene glycol (EG) is used as the solvent and reducing agent to reduce AgNO_3 to AgNWs. The key factors for synthesizing high-aspect-ratio AgNWs are slow nucleation, rapid growth, and deoxygenation. To regulate AgNW growth, the length and diameter of the AgNWs are tuned by changing the molecular weight of PVP, controlling the concentration of the additives, or varying the type of agent used (such as those containing Fe^{3+} , Cu^{2+} , Cl^- , and Br^- ions) [28–31]. Increasing the aspect ratio of AgNWs further via polyol processing is an appealing but challenging strategy. Wang et al. [28] reported that the aspect ratio of AgNWs prepared in a Br^- – Cl^- mixed solution was much higher than those of AgNWs prepared in both, a single Br^- solution and a single Cl^- solution. Similarly, by adjusting the $\text{Cu}^{2+}/\text{Fe}^{3+}$ molar ratio, Mao et al. [32] obtained AgNWs with a diameter of 30 nm and aspect ratio of up to 4000.

It has been reported that the metal cations introduced into the polyol system act as redox pairs (such as $\text{Fe}^{3+}/\text{Fe}^{2+}$ and $\text{Cu}^{2+}/\text{Cu}^+$) and prevent oxidative etching, thereby improving the selectivity and uniformity of the formed AgNWs. Here, we report the one-step synthesis of ultrahigh-aspect-ratio AgNWs (diameter of 40 nm and aspect ratio of 2000) by controlling the total molar concentration of Cl^- in the reaction solution (concentration of Cl^- was 420 μM in 75 mL of the

reaction solution) to adjust the $\text{Cu}^{2+}/\text{Fe}^{3+}$ molar ratio. This method does not require a protective gas during synthesis, and the process time does not exceed 2 h. The synthesized AgNWs were finally transferred to plastic substrates (polyethylene terephthalate (PET)) by the coating method to fabricate AgNW-hydroxyethyl cellulose (HEC) FTCFs, which showed a low sheet resistance (68 Ω/sq) and high transmittance (86.70% at 550 nm).

2 Experimental

2.1 Materials

All chemical reagents were of analytical grade and used without further purification. These included silver nitrate (AgNO_3 , $\geq 99.8\%$, Sinopharm), EG ($\geq 99.0\%$, Sinopharm), acetone ($\text{C}_3\text{H}_6\text{O}$, $\geq 99.5\%$, Sinopharm), PVP ($M_w \approx 1,300,000$, Aldrich), ferric chloride hexahydrate ($\text{FeCl}_3 \cdot 6\text{H}_2\text{O}$, $\geq 99.5\%$, Sinopharm), copper chloride dihydrate ($\text{CuCl}_2 \cdot 2\text{H}_2\text{O}$, $\geq 99.5\%$, Sinopharm), sodium bromide (NaBr , $\geq 99.5\%$, Sinopharm), HEC (Aldrich), and ethanol ($\text{C}_2\text{H}_5\text{OH}$, $\geq 99.0\%$, Xilong Chemicals). Deionized water with a resistivity of 18.2 M Ω cm was obtained using a purification system.

2.2 Synthesis of AgNWs

Ultralong AgNWs were synthesized by a one-step chemical reaction. Firstly, 1.2 g of PVP ($M_w \approx 1,300,000$) was dissolved in 50 mL of EG. Next, the solution was heated and continuously stirred at 170 °C for 1 h. Subsequently, when the Cl^- ion concentration was 420 μM (total volume = 75 mL), EG containing FeCl_3 and CuCl_2 was added in a certain proportion to the PVP solution. Simultaneously, 10 mL of a NaBr solution (1.05 mM) was added to the mixture, and the mixture was stirred for 15 min at 170 °C. Finally, 10 mL of AgNO_3 (0.6 M) was added to the mixture and stirred at 170 °C for 45 min. The solution was then cooled to room temperature.

After completion of the reaction, the solution was added to acetone for rapid precipitation, following which the supernatant was removed, dispersed in ethanol, and washed. After repeating the reaction 3 times, pure AgNWs with ultrahigh aspect ratios were obtained. Finally, the AgNWs were dispersed in ethanol. A schematic representation of the synthesis process and the changes in the color of the reaction

solution during the procedure are shown in Fig. 1a and b.

2.3 Fabrication of AgNW-HEC FTCFs

AgNW (10 mg/mL) and HEC (8 mg/mL) solutions were mixed in a 1:1 ratio and stirred for 1 h to obtain a AgNW conductive ink. A slit coater (Ossila L2005, UK) coated with the AgNW conductive ink was used to form films on PET substrates [33]. First, the ink was injected, and a coating was formed at a speed of 3–8 mm/s, ink flow rate of 0.5–2.5 mL/min, and substrate temperature of 50 °C. The coated AgNW film was subsequently dried in an oven at 130 °C for 30 min to improve the wire–wire connections. A photograph of the thus-prepared film is shown in Fig. 5d. It can be seen that the FTCFs based on the AgNWs exhibit high transmittance.

2.4 Structural characterization and property analysis

The surface morphology of the AgNWs was characterized using field-emission scanning electron microscopy (FESEM, Hitachi S-4800, Japan) and high-resolution transmission electron microscopy (HRTEM, Talos F200X, USA). X-ray diffraction (XRD) analysis (DX-2700BH, China) was performed at a scan rate of 4°/min using a Cu-K α radiation source ($\lambda = 1.54056$

Å) to analyze the structure and crystallinity of the AgNWs. The ultraviolet-visible (UV–Vis) spectrum of the AgNWs and the optical transmittance of the AgNWs-HEC FTCFs were measured using a UV–Vis–near infrared spectrophotometer (Shimadzu UV-2600, Japan). The sheet resistances of the AgNW-HEC FTCFs were evaluated using a four-point probe system (SM-4, China). Finally, their mechanical robustness was analyzed using a laboratory-manufactured system.

3 Results and discussion

The aspect ratio of the synthesized AgNWs varied with the Cu²⁺/Fe³⁺ molar ratio, and typical AgNWs synthesized at a Cu²⁺/Fe³⁺ molar ratio of 5:2 exhibited the highest aspect ratio. Table 1 shows the average length, diameter, and aspect ratio of AgNWs formed using different experimental parameters.

The products were also characterized using HRTEM and selected-area electron diffraction (SAED) analyses. A typical TEM image of sample AgNW-1 is shown in Figs. 2a and S1; the diameter of the AgNWs is approximately 40 nm. Figure 2b shows an HRTEM image of typical AgNWs. The NWs are highly crystalline with an estimated lattice plane spacing of 0.24 nm, which is consistent with the separation between the (111) planes of Ag. The growth direction of the AgNWs is perpendicular to the plane. The corresponding SAED

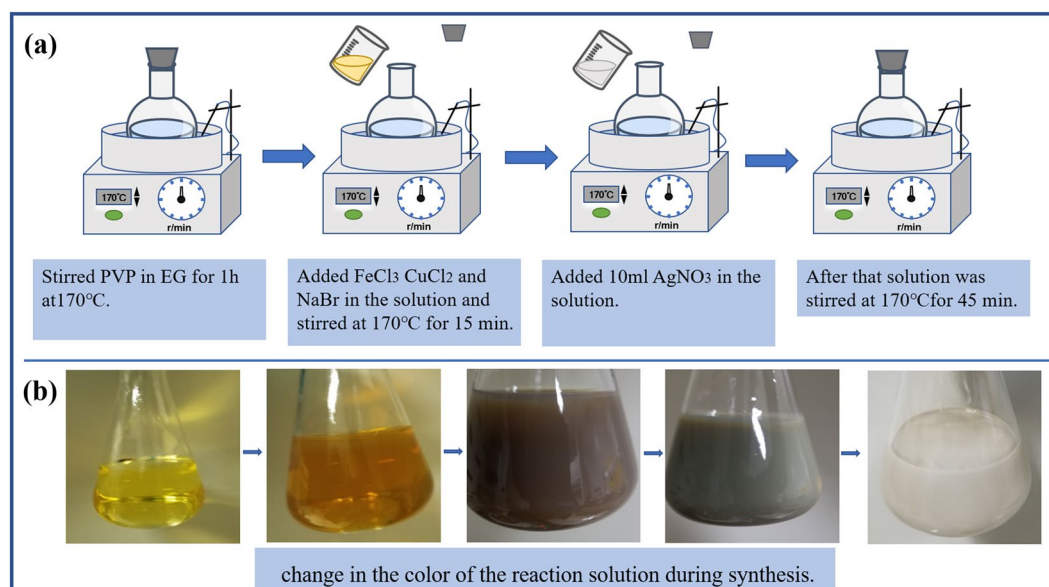
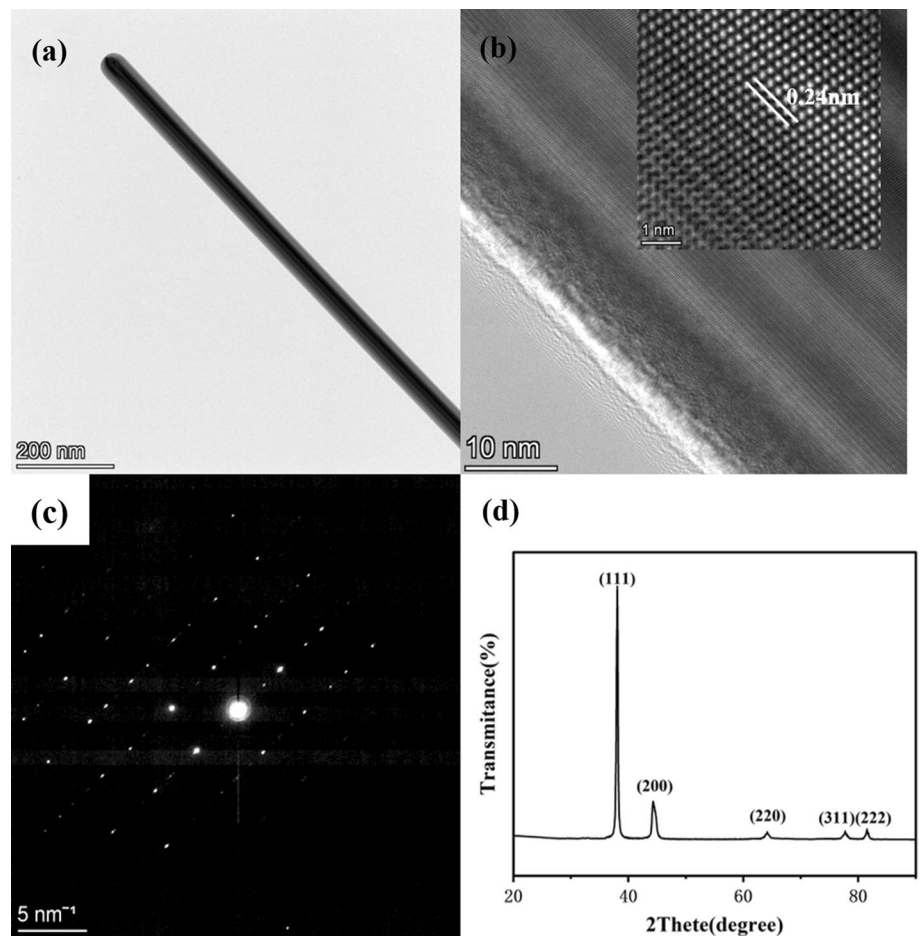


Fig. 1 **a** Schematic of experimental procedure for the synthesis of AgNWs. **b** change in the color of the reaction solution during synthesis

Table 1 Average length, diameter, and aspect ratio of AgNWs formed using different experimental parameters

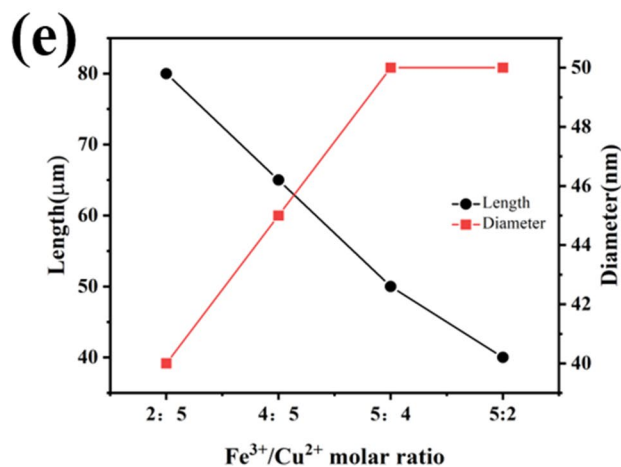
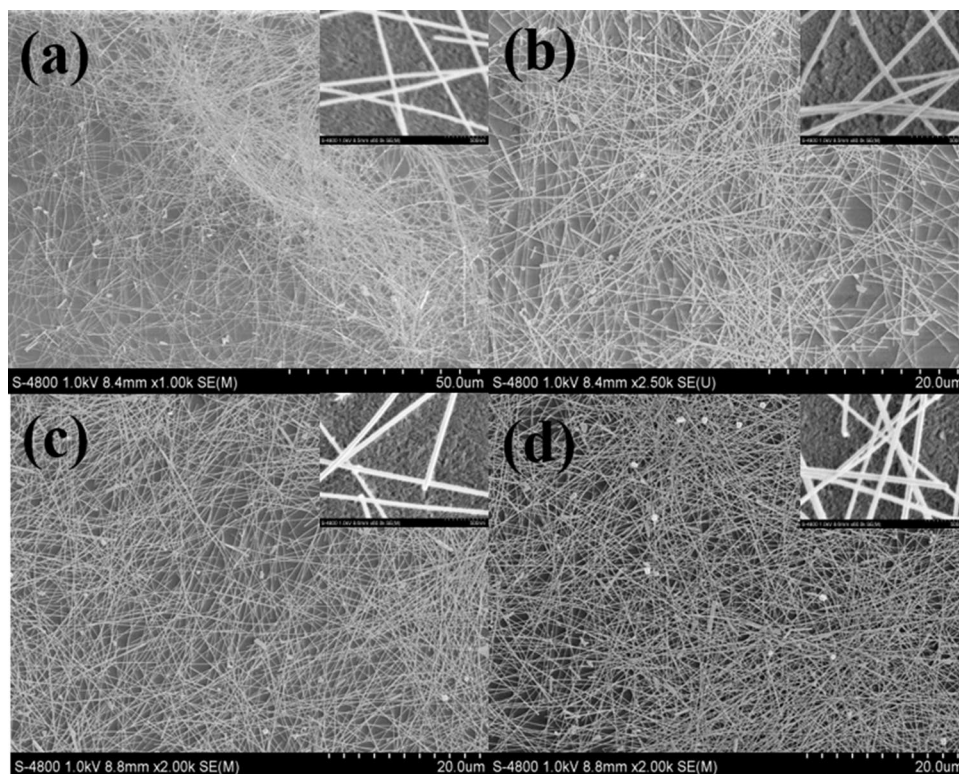
Sample (Fe ³⁺ /Cu ²⁺)	FeCl ₃ /1 mL (mM)	CuCl ₂ /1 mL (mM)	NaBr/1 mL (mM)	L (μm)	D (nm)	AR(L/D)
1 (2:5)	3.9	9.8	10.5	80 ± 20	40 ± 10	2000
2 (4:5)	5.7	7.2	10.5	65 ± 20	45 ± 10	1444
3 (5:4)	6.9	5.5	10.5	50 ± 20	50 ± 10	1000
4 (5:2)	8.3	3.3	10.5	40 ± 20	50 ± 10	800
5 (2:5)	3.9	9.8	0	20 ± 20	190 ± 20	105
6 (2:5)	3.9	9.8	31.5	30 ± 20	45 ± 10	667

Fig. 2 a TEM. b HRTEM. c SAED. d XRD patterns of synthesized AgNWs

pattern confirms the single-crystalline nature of the AgNWs (Fig. 2c). Figure 2d shows the XRD pattern of typical AgNWs. The diffraction peaks can be indexed to the (111), (200), (220), (311), and (222) planes of the pure face-centered cubic silver crystal; the peak widths are small, indicating that the AgNWs have a high crystallinity. This is consistent with the data in JCPDS Card No. 04-0783. Finally, no peaks related to impurities are detected, indicating the formation of high-purity AgNWs.

Figure 3 shows SEM images of the AgNWs synthesized using different Cu²⁺/Fe³⁺ molar ratios. First, we increased the Cu²⁺ ion concentration during preparation. As the concentration of Cu²⁺ was increased, the average length of the AgNWs increased from 40 μm to 3.3 mM to 80 μm at 9.8 mM. This suggests that a high concentration of Cu²⁺ ions is beneficial for forming ultralong AgNWs. However, the amount of the byproduct, namely, Ag nanoparticles, increased with increasing Cu²⁺ concentration. Note that when the

Fig. 3 SEM images of AgNWs synthesized using different $\text{Cu}^{2+}/\text{Fe}^{3+}$ molar ratios. **a** 5:2. **b** 5:4. **c** 4:5. **d** 2:5. **e** Changes in AgNWs diameter and length with $\text{Cu}^{2+}/\text{Fe}^{3+}$ molar ratios



molar ratio of $\text{Cu}^{2+}/\text{Fe}^{3+}$ was 5:2, although the AgNWs were the longest, the amount of the byproduct (Ag nanoparticles) formed was the largest.

When preparing high-aspect-ratio AgNWs, it is not only important to form NWs of a suitable size and high aspect ratio, but also necessary to ensure that the NWs are highly pure and free from contamination. This is because the aspect ratio of the AgNWs and presence of nanoparticle-sized impurities significantly affect the conductivity and transparency of the NW network. In this study, the uniformity of the AgNWs was studied

while changing the $\text{Cu}^{2+}/\text{Fe}^{3+}$ molar ratio because Fe^{3+} ions can affect the uniformity and morphology of the AgNWs. As shown in Figs. 3a and S2, uniform AgNWs with a diameter of 40 nm and an ultrahigh aspect ratio of up to 2000 are obtained at a $\text{Cu}^{2+}/\text{Fe}^{3+}$ molar ratio of 5:2. When the molar ratio of $\text{Cu}^{2+}/\text{Fe}^{3+}$ is 5:4 (Fig. 3b), the average length of the AgNWs is 65 μm , the diameter is approximately 45 nm, and there are many impurities. In addition, when the molar ratio of $\text{Cu}^{2+}/\text{Fe}^{3+}$ is reduced to 4:5 and 2:5 (Fig. 3c and d), fewer nanoparticles are formed as impurities in the reaction

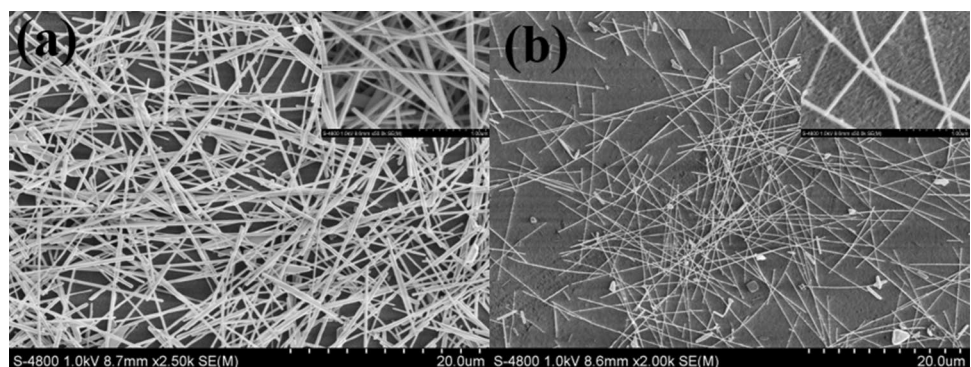
product, and the diameter of the AgNWs increases to 50 nm. The diameter and length of AgNWs varying with $\text{Cu}^{2+}/\text{Fe}^{3+}$ molar ratio concentration is illustrated in Fig. 3e. The experimental results presented in Fig. 3 suggest that even when the Fe^{3+} ions are present in a trace amount, etching occurs to some degree, and this etching effect is greatly enhanced with an increase in the concentration of Fe^{3+} ions. This, in turn, strongly affects the morphology of the AgNWs. The oxidation-etching effect of Fe^{3+} is greater than that of Cu^{2+} . The addition of Fe^{3+} ions facilitates the growth of multiple twinned seeds for the formation of NWs by removing oxygen from the surface of the twinned seeds and preventing their dissolution by oxidative etching. Therefore, when the $\text{Cu}^{2+}/\text{Fe}^{3+}$ ratio is increased to 4:5, the purity of the AgNWs is the highest, and the concentration of the Ag nanoparticles is the lowest. Intriguingly, when the $\text{Cu}^{2+}/\text{Fe}^{3+}$ ratio is increased to 2:5, spherical nanoparticles, polyhedral, and nanorods are formed because of the excessive Fe^{3+} ions. Thus, moderate amounts of Cu^{2+} and Fe^{3+} ions synergistically facilitate the formation of AgNWs with high purity and aspect ratios.

The physicochemical properties of AgNWs play an important role in determining their growth behavior. Br^- and Cl^- ions promote the adhesion of halogen ions onto the surfaces of AgNWs, promoting their growth and crystallinity. When the molar ratio of $\text{Cu}^{2+}/\text{Fe}^{3+}$ is 5:2, the Br^- ion concentration is 0 mM, the average length of the AgNWs is 20 μm , and their diameter is approximately 190 nm (Fig. 4a). However, when the concentration of Br^- is increased to 31.5 mM, the average length of the AgNWs changes from 20 to 30 μm , as shown in Fig. 4b. With the addition of Br^- ions in the

appropriate concentration, the diameter of the AgNWs decreases significantly from 190 to 40 nm, and their length increases from 20 to 80 nm. Because of the selective etching effect of the Br^- ions, their addition in the appropriate concentration can promote the formation of AgNWs; however, when the Br^- ion concentration is too high, the release rate of the Ag^+ ions is too low, resulting in the growth of multiple double seeds into the AgNWs that are strongly etched by Br^-/O_2 .

Moreover, the conductivity and transmittance of the synthesized AgNW-HEC films have a determining effect on their commercial applicability. In this study, PET films were used as the substrates, resulting in the AgNW-HEC films exhibiting different sheet resistances and light transmittances (Fig. 5a). The transmittances of the films at 550 nm with sheet resistances of 68 and 15 Ω/sq were 86.70 and 82.05%, respectively. Its sheet resistance after the folding-relaxation cycles is shown in Fig. 5b. No degradation is observed during the first 1200 folding cycles. Thereafter, the sheet resistance slowly increases with folding, and after 3000 folding cycles, the sheet resistance increases from 68 to 70 Ω/sq . The net increase is only 3.15%. Next, the conductivity of the FTCFs was confirmed by inserting an FTCF with a sheet resistance of 68 Ω/sq in a circuit (red dashed circle), as shown in Fig. 5c, and turning on the light-emitting diode. Figure 5d shows a photograph of a representative AgNW-HEC conductive thin film. The experiment results on atmospheric degradation behavior of the film were shown in Figs. S3 and S4. Based on the results of this study, it can be concluded that AgNW-HEC conductive films are promising materials with high conductivity and foldability for use in the electronics industry.

Fig. 4 SEM images of AgNWs synthesized at a $\text{Cu}^{2+}/\text{Fe}^{3+}$ molar ratio of 5:2 when the Br^- concentration is **a** 0 mM and **b** 8 mM



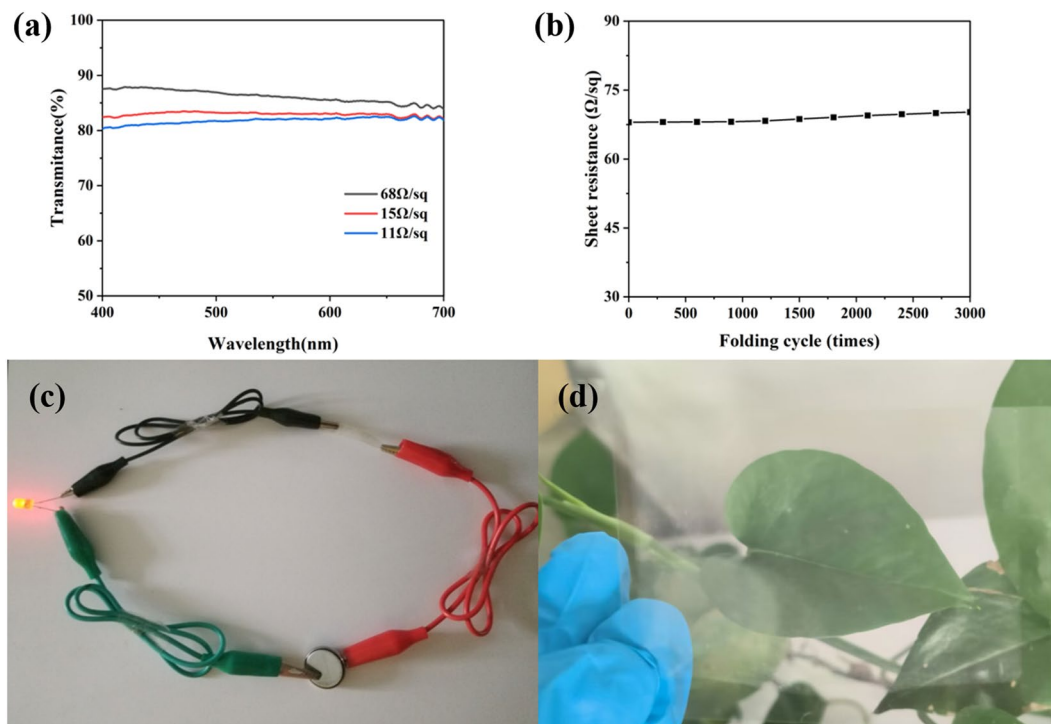


Fig. 5 **a** Transmittance of AgNWs-HEC film fabricated in this work. **b** changes in the sheet resistance of the AgNW-HEC conductive thin film during 3000 cycles of folding. **c** turning on of

a light-emitting diode using a AgNW-based electrode. **d** photograph of a AgNW-HEC film prepared by coating

4 Conclusions

In summary, we synthesized ultralong AgNWs with aspect ratios higher than 2000. The average diameter of these AgNWs was 40 nm and their average length was approximately 80 μm , which is greater than that of normal AgNWs (typically, the aspect ratio of AgNWs is approximately 1000). The successful fabrication of the ultralong AgNWs was achieved by controlling the $\text{Cu}^{2+}/\text{Fe}^{3+}$ molar ratio during the formation reaction. Subsequently, a simple coating method was used to prepare AgNW-HEC FTFCs with a sheet resistance of 68 Ω/sq and transmittance of 86.70% at 550 nm. Even after 3000 bending tests, the sheet resistance of these films changed only slightly, indicating that the fabricated AgNWs are highly suitable for preparing transparent conductive films.

Acknowledgements

This work is supported by the Science and Technology Project of Jiaying (2022AY10005); Science and Technology Project of Jiaying (2019AY11018); General scientific

research project of Zhejiang Education Department (Y202250333).

Author contributions

HZA: investigation, data curation, writing-original draft preparation, writing-review and editing, formal analysis. JYF: conceptualization, investigation, methodology, validation, data curation, writing-review and editing, resources, supervision, project administration. PC: investigation, data curation, formal analysis. TY: investigation, data curation, formal analysis. TS: formal analysis. BX: review and editing, formal analysis, funding acquisition.

Funding

This research is funded by the Science and Technology Project of Jiaying (2022AY10005); Science and Technology Project of Jiaying (2019AY11018); General scientific research project of Zhejiang Education Department (Y202250333).

Data availability

Data and materials will be made available on request.

Code availability

Not applicable.

Declarations

Conflict of interest No potential conflict of interest was reported by the authors.

Ethical approval Not applicable.

Consent to participate Not applicable.

Consent for publication Informed consent.

Supplementary Information The online version contains supplementary material available at <https://doi.org/10.1007/s10854-023-11579-0>.

References

1. L. Lin, Y. Choi, T. Chen, H. Kim, K.S. Lee, J.M. Kang, L. Lyu, J.F. Gao, Y. Piao, Superhydrophobic and wearable TPU based nanofiber strain sensor with outstanding sensitivity for high-quality body motion monitoring. *Chem. Eng. J.* **419**, 129513 (2021)
2. A.R. Madaria, A. Kumar, C. Zhou, Large scale, highly conductive and patterned transparent films of silver nanowires on arbitrary substrates and their application in touch screens. *Nanotechnology* **22**, 245201 (2011)
3. A. Moradi, M. Abrari, M. Ahmadi, Efficiency enhancement in dye-sensitized solar cells through the decoration of electro-spun TiO₂ nanofibers with ag nanoparticles. *J. Mater. Sci. Mater. Electron.* **31**, 16759–16768 (2020)
4. Z.-R. Zhu, W. Geng, Q. Zhu, A.S. Ethiraj, T. Wang, L.-C. Jing, Y.-J. Ning, Y. Tian, W.-H. Geng, L. Wu, H.-Z. Geng, Highly transparent, low sheet resistance and stable tannic acid modified-SWCNT/AgNW double-layer conductive network for organic light emitting diodes. *Nanotechnology* **32**, 015708 (2021)
5. H. Lee, D. Lee, Y. Ahn, E.-W. Lee, L.S. Park, Y. Lee, Highly efficient and low voltage silver nanowire-based OLEDs employing a n-type hole injection layer. *Nanoscale* **6**, 8565–8570 (2014)
6. W. Dong, C. Zhu, W. Hu, L. Xiao, Y. Huang, Stretchable human-machine interface based on skin-conformal sEMG electrodes with self-similar geometry. *J. Semicond.* **39**, 014001–014001 (2018)
7. M. Saychak, N. Borodinov, R. Burtovyy, M. Anayee, K. Hu, R. Ma, A. Grant, H. Li, D.B. Cutshall, Y. Wen, G. Koley, W.R. Harrell, G. Chumanov, V. Tsukruk, I. Luzinov, Highly conductive and transparent reduced graphene oxide nanoscale films via thermal conversion of polymer-encapsulated graphene oxide sheets. *ACS Appl. Mater. Interfaces* **10**, 3975–3985 (2018)
8. D.H. Shin, S.W. Seo, J.M. Kim, H.S. Lee, S.-H. Choi, Graphene transparent conductive electrodes doped with graphene quantum dots-mixed silver nanowires for highly-flexible organic solar cells. *J. Alloys Compd.* **744**, 1–6 (2018)
9. Y. Chen, X.-Y. Fu, Y.-Y. Yue, N. Zhang, J. Feng, H.-B. Sun, Flexible and transparent supercapacitor based on ultrathin Au/graphene composite electrodes. *Appl. Surf. Sci.* **467**, 104–111 (2019)
10. J. Ning, L. Hao, M. Jin, X. Qiu, Y. Shen, J. Liang, X. Zhang, B. Wang, X. Li, L. Zhi, A facile reduction method for roll-to-roll production of high performance graphene-based transparent conductive films. *Adv. Mater.* **29**, 1605028 (2017)
11. A.A. Tonkikh, V.I. Tsebro, E.A. Obraztsova, D.V. Rybkovskiy, A.S. Orekhov, I.I. Kondrashov, E.I. Kauppinen, A.L. Chuvilin, E.D. Obraztsova, Films of filled single-wall carbon nanotubes as a new material for high-performance air-sustainable transparent conductive electrodes operating in a wide spectral range. *Nanoscale* **11**, 6755–6765 (2019)
12. O. Urper, I. Cakmak, N. Karatepe, Fabrication of carbon nanotube transparent conductive films by vacuum filtration method. *Mater. Lett.* **223**, 210–214 (2018)
13. P. Zhao, Q. Tang, X. Zhao, Y. Tong, Y. Liu, Highly stable and flexible transparent conductive polymer electrode patterns for large-scale organic transistors. *J. Colloid Interface Sci.* **520**, 58–63 (2018)
14. J. Yang, C.X. Bao, K. Zhu, T. Yu, Q.Y. Xu, High-performance transparent conducting metal network electrodes for perovskite photodetectors. *ACS Appl. Mater. Interfaces* **10**, 1996–2003 (2018)
15. X.S. Li, Y.M. Wang, C.R. Yin, Z.X. Yin, Copper nanowires in recent electronic applications: progress and perspectives. *J. Mater. Chem. C* **8**, 849–872 (2020)
16. Y. Li, Y. Li, Z. Fan, H. Yang, X. Yuan, C. Wang, Ascorbic acid-assisted one-step chemical reaction to design an ultra-long silver nanowire structure for a highly transparent flexible conducting Film. *ACS Omega* **5**, 18458–18464 (2020)

17. J. Lee, P. Lee, H.B. Lee, S. Hong, I. Lee, J. Yeo, S.S. Lee, T.S. Kim, D. Lee, S.H. Ko, Room-temperature nanosoldering of a very long metal nanowire network by conducting-polymer-assisted joining for a flexible touch-panel application. *Adv. Funct. Mater.* **23**, 4171–4176 (2013)
18. R.M. Mutiso, M.C. Sherrott, A.R. Rathmell, B.J. Wiley, K.I. Winey, Integrating simulations and experiments to predict sheet resistance and optical transmittance in nanowire films for transparent conductors. *ACS Nano* **7**, 7654–7663 (2013)
19. R.R. da Silva, M. Yang, S.-I. Choi, M. Chi, M. Luo, C. Zhang, Z.-Y. Li, P.H.C. Camargo, S.J. Lima Ribeiro, Y. Xia, Facile synthesis of Sub-20 nm silver nanowires through a bromide-mediated polyol method. *ACS Nano* **10**, 7892–7900 (2016)
20. Z. Chen, J.W. Chang, C. Balasanthiran, S.T. Milner, R.M. Rioux, Anisotropic growth of silver nanoparticles is kinetically controlled by polyvinylpyrrolidone binding. *J. Am. Chem Soc* **141**, 4328–4337 (2019)
21. Y.G. Sun, Y.D. Yin, B.T. Mayers, T. Herricks, Y.N. Xia, Uniform silver nanowires synthesis by reducing AgNO₃ with ethylene glycol in the presence of seeds and poly(vinyl pyrrolidone). *Chem. Mater.* **14**, 4736–4745 (2002)
22. M. Jia-qing, H. Jun-wei, Template-directed synthesis of Ag nanowire arrays by a simple paired cell method for SERS. *Optoelectron. Lett.* **11**, 401–404 (2015)
23. X.J. Xu, G.T. Fei, X.W. Wang, Z. Jin, W.H. Yu, L.D. Zhang, Synthetic control of large-area, ordered silver nanowires with different diameters. *Mater. Lett.* **61**, 19–22 (2007)
24. L. Lin, L. Liu, P. Peng, G. Zou, W.W. Duley, Y.N. Zhou, In situ nanojoining of Y- and T-shaped silver nanowires structures using femtosecond laser radiation. *Nanotechnology* **27**, 125201 (2016)
25. Y. Chen, Y. Zhang, J. Chen, X. Sun, Understanding the influence of crystallographic structure on controlling the shape of noble metal nanostructures. *Cryst. Growth Des.* **11**, 5457–5460 (2011)
26. W.C. Zhang, X.L. Wu, H.T. Chen, Y.J. Gao, J. Zhu, G.S. Huang, P.K. Chu, Self-organized formation of silver nanowires, nanocubes and bipyramids via a solvothermal method. *Acta Mater.* **56**, 2508–2513 (2008)
27. Y.G. Sun, B. Mayers, T. Herricks, Y.N. Xia, Polyol synthesis of uniform silver nanowires: a plausible growth mechanism and the supporting evidence. *Nano Lett.* **3**, 955–960 (2003)
28. X.-M. Wang, L. Chen, E. Sowade, R.D. Rodriguez, E. Sheremet, C.-M. Yu, R.R. Baumann, J.-J. Chen, Ultra-uniform and very thin Ag nanowires synthesized via the synergy of Cl⁻, Br⁻ and Fe³⁺ for transparent conductive films. *Nanomaterials* **10**, 237 (2020)
29. J.-J. Chen, S.-L. Liu, H.-B. Wu, E. Sowade, R.R. Baumann, Y. Wang, F.-Q. Gu, C.-R.-L. Liu, Z.-S. Feng, Structural regulation of silver nanowires and their application in flexible electronic thin films. *Mater. Des.* **154**, 266–274 (2018)
30. K. Zhan, R. Su, S. Bai, Z. Yu, N. Cheng, C. Wang, S. Xu, W. Liu, S. Guo, X.-Z. Zhao, One-pot stirring-free synthesis of silver nanowires with tunable lengths and diameters via a Fe³⁺ & Cl⁻ co-mediated polyol method and their application as transparent conductive films. *Nanoscale* **8**, 18121–18133 (2016)
31. N. Xiao, Y. Chen, W. Weng, X. Chi, H. Chen, D. Tang, S. Zhong, Mechanism understanding for size regulation of silver nanowires mediated by halogen ions. *Nanomaterials* **12**, 2681 (2022)
32. Y. Mao, H. Yang, C. Hu, J. Guo, X. Meng, Y. Yang, Large-scale synthesis of AgNWs with ultra-high aspect ratio above 4000 and their application in conductive thin film. *J. Mater. Sci. Mater. Electron.* **28**, 5308–5314 (2017)
33. C. Liu, X. Zhang, J. Shan, Z. Li, X. Guo, X. Zhao, H. Yang, Large-scale preparation of silver nanowire-based flexible transparent film heaters by slot-die coating. *Materials* **15**, 2634 (2022)

Publisher's Note Springer Nature remains neutral with regard to jurisdictional claims in published maps and institutional affiliations.

Springer Nature or its licensor (e.g. a society or other partner) holds exclusive rights to this article under a publishing agreement with the author(s) or other rightsholder(s); author self-archiving of the accepted manuscript version of this article is solely governed by the terms of such publishing agreement and applicable law.